Reference: *Biol. Bull.* **192**: 375–387. (June, 1997)

Post-Hatching Development of Circular Mantle Muscles in the Squid *Loligo opalescens*

THOMAS PREUSS, ZORA N. LEBARIC, AND WILLIAM F. GILLY

Hopkins Marine Station, Department of Biological Sciences, Stanford University, Pacific Grove, California 93950

Abstract. Post-hatching development of the circular muscles in the mantle of squid was studied morphometrically to identify structural changes and to quantify hyperplasia and hypertrophy of the muscle fibers. Superficial, mitochondria-rich (SMR) fibers and central, mitochondria-poor (CMP) fibers are present at hatching. Although both fiber types increase in size and, even more so, in number during post-hatching development, CMP fibers increase at a much higher rate than do SMR fibers. As a result, the relative proportion of SMR to CMP fibers shifts from about 1:1 in a hatchling to about 1:6 in an 8-week-old animal; it then apparently remains constant to adulthood. These structural changes are consistent with developmental changes in muscular activity. During slow, jet-propelled swimming, 1-week-old animals show mantle contractions that have twice the relative amplitude and frequency of those in adults. The presence of Na-channel protein in mantle muscle was detected biochemically by using site-directed antibodies; the protein was found to be preferentially expressed in CMP fibers. These results suggest that SMR fibers are an important source of locomotory power at hatching, but become progressively less important during the first 8 weeks of development as CMP fibers assume the dominant role in jet locomotion.

Introduction

Jet propulsion in squids is caused by the antagonistic action of circular and radial mantle muscles in connection with two layers of stiff, collagenous tunics and a network of intermuscular connective tissue fibers (Ward and Wainwright, 1972; Bone *et al.*, 1981; Gosline *et al.*, 1983; Kier, 1988; Wells, 1988). The circular muscle mass, responsible for producing thrust during jet propulsion, is divided into three layers, largely on the basis of the relative mitochondrial content of individual muscle fiber types. Two thin layers of superficial mitochondria-rich, oxidative fibers on the outer and inner mantle surface enclose a much thicker layer of mitochondria-poor, glycolytic fibers in the central zone (Bone *et al.*, 1981; Mommsen *et al.*, 1981). In light of these structural and metabolic differences, it has been proposed that the superficial layers are active during respiration and slow jet-propelled swimming, whereas the central circular fibers, presumed to be innervated by the giant axon system, power the jet-escape and rapid locomotion (Bone *et al.*, 1995). In general agreement with these ideas, recent electrophysiological studies have revealed that at least two classes of circular muscle fibers can be distinguished on the basis of their electrical properties and that some of the circular fibers, presumably those innervated by giant axons, display Na-channel-based excitability (Gilly *et al.*, 1996).

Jet propulsion, mantle mechanics, and mantle structure have been well studied in adult squid, but relevant work on hatchlings and developing juvenile squid is comparatively limited (Zuev, 1966; v. Boletzky, 1982, 1987; O'Dor *et al.*, 1986; Moltschaniwskyj, 1994, 1995; Matsuno, 1987). Although squid begin actively swimming by jet propulsion as soon as they hatch (Packard, 1969), the full flexibility and fine coordination of the locomotor system is lacking (Gilly *et al.*, 1991; Chen *et al.*, 1996). The aim of the present study was to analyze the maturation of the mantle musculature during post-

Received 2 December 1996; accepted 3 April 1997.

Abbreviations: CMP = central mitochondria-poor muscle fibers; DML = dorsal mantle length; GFL = giant fiber lobe; SMR = superficial mitochondria-rich muscle fibers; SR = sarcoplasmic reticulum.

hatching development and to identify structural and functional characteristics of the different types of muscle fiber associated with jet-propelled locomotion. In pursuit of that goal, we combined three approaches. First, anatomical and morphometric methods at light- and electron-microscopic levels were used to reveal structural changes as squid mature from hatchlings to adults. Second, the kinematics of mantle contractions in free-swimming animals were investigated to shed light on functional characteristics of locomotion at different maturity stages. Third, biochemical analysis of the presence of Na-channel protein in superficial and central fibers provided a tool to characterize the location and abundance of putative fast-twitch fibers in the developing mantle musculature.

Our results indicate that superficial, mitochondria-rich (SMR) fibers are an important source of locomotory power at hatching but become progressively less important during the first 8 weeks after hatching. Over this same period, central, mitochondria-poor (CMP) fibers increase in number until they contribute most of the overall mantle muscle mass and play the dominant role in jet locomotion.

Materials and Methods

Experimental animals

Loligo opalescens was collected in Monterey Bay, California, between August and November of 1995. Animals were maintained at Hopkins Marine Station in circular tanks (2.5 m diameter; 1 m deep) plumbed with flow-through natural seawater. Spawning typically occurred in these tanks within 3–5 days of collecting the squid. Clusters of egg cases were removed and cultured at the Monterey Bay Aquarium, Monterey, California, in flow-through circular 320-l tanks (temperature range 13–16°C) until natural hatching occurred. During the first 10 weeks, squid received a diet, *ad libitum*, of brine shrimp nauplii (*Artemia salina*) enriched with algae and Super Selco (a nutrient medium rich in lipids, fatty acids, and vitamins; produced by Artemia Systems N. V., Belgium). Copepods (*Acartia* sp.) and mysids (*Acanthomysis* sp.) were added to the diet when available (about twice per week).

Mantle anatomy

The anatomy of the mantle musculature was examined by light microscopy (LM) and transmission electron microscopy (TEM). Prior to dissection, all animals were anesthetized for 20 min in 7.5% $MgCl_2$ diluted 1:1 in oxygenated seawater and then killed by decapitation. Tissue for fixation was removed from adult squid within 1 day after collection. Blocks of mantle muscle were cut parallel to the main body axis and taken from an anterodorsal region close to the stellate ganglion of five adults with dorsal mantle lengths (DML) between 80 and 140 mm. For studies of hatchling and juvenile squid, six healthy looking animals that displayed vigorous swimming capability were collected for fixation weekly over a 10-week period. These animals were fixed whole, and smaller tissue samples for ultrastructural analysis of the mantle muscles were taken after fixation. In all animals (except hatchlings), the skin was carefully removed before fixation.

For LM, the tissue was fixed in 4% paraformaldehyde in filtered seawater for 3–5 days at 4°C, dehydrated in graded ethanol, and either infiltrated with paraffin under vacuum or embedded in plastic (JB4; Polysciences, Inc.). Thick sections (6–10 μm) and semithick sections (2–4 μm) were cut and stained with conventional histological stains and viewed with an Olympus BH-2 microscope.

For TEM, the tissue samples were fixed in 0.065 *M* sodium phosphate buffer (pH 7.4) with 3% glutaraldehyde, 0.5% tannic acid, and 6% sucrose for 8 h at 4°C (first 15 min at room temperature), rinsed in 0.065 *M* sodium phosphate buffer without sucrose, and postfixed in a 1:1 mix of 0.13 *M* cacodylate buffer (pH 7.2) with 2% potassium ferrocyanide and 2% osmium tetroxide for 40 min at 4°C. Thereafter, the tissue was rinsed in 0.065 *M* cacodylate buffer, dehydrated in graded ethanol, and infiltrated overnight (10–12 h) in resin (LR White; Sigma). For sectioning, the blocks were oriented to obtain transverse, sagittal, and tangential sections of the circular mantle muscles. Thin (0.8–1 μm) and ultrathin (gray-silver) sections were obtained in alternating section series, thereby collecting ultrathin sections every 4–6 μm in hatchlings and juveniles and every 50–60 μm in adults. Up to five consecutive section series were collected in this manner. Thin sections were stained with toluidine blue and examined with an Olympus BH-2 microscope. Ultrathin sections were collected onto Formvar-coated mesh and slot grids (Electron Microscopy Sciences), stained either with a saturated aqueous uranyl acetate solution and Reynolds' lead citrate or with 2% phosphotungstic acid, and examined with Phillips EM 201 or EM 401 electron microscopes. The magnification stops were calibrated with a diffraction grating replica (Ted Pella, Inc.).

For morphometric analysis of the muscle fibers, a computer-aided image analysis program (NIH-Image 1.60) was used on a Power Macintosh 7100/80 computer. TEM micrographs of muscle fibers were digitized at 600-dpi resolution using a scanner (Microtek ScanMaker II_{HR}), and stored on a magneto-optical drive (Pin-

nacle Tahoe 230 MB). In addition, LM video-images were obtained using an Olympus BH-2 microscope equipped with a CCD B/W camera (Sony SSC-M374), and selected frames were digitized with a high-resolution video capture card (Scion LR-3).

Measurements were taken on longitudinal mantle sections (*i.e.*, on a cross section of the circular muscle fibers). Two measurements of each muscle fiber visible in a given electron micrograph were taken: (i) the total cross-sectional area of a single muscle fiber and (ii) the area occupied by its mitochondrial core. The difference between these values approximates the remaining myofilament area; this value also includes cytoplasm and sarcoplasmic reticulum (SR). Additional measurements were taken in selected micrographs to determine the cross-sectional area (and the calculated diameter) of synaptic vesicles in nerve processes.

Mantle kinematics

A dorsal view of freely swimming juvenile (1-week-old) and adult squid in their respective holding and rearing tanks was filmed with a high-resolution CCD B/W video camera (Sony SSC-M374) mounted above the tanks on a remote controlled panning motor (Prinz Power-Panner 430-62), and recorded on a Sony Hi-8 recorder (EVO-9700). Single video-frame analysis of digitized video sequences was carried out using the image analysis system described above. The mantle diameter was measured at its widest point (the anterior mantle end in juveniles and about $^1/_3$ from the anterior mantle end in adults) in successive, enlarged video images (calibrated by dorsal mantle length). To compare mantle diameter dimensions in animals of different size, the fractional mantle diameter was calculated by defining the largest diameter in a given measurement sequence as 100%.

Biochemistry

Production of antibodies. Two antibodies (one polyclonal and one monoclonal) directed against distinct regions of a putative squid sodium channel encoded by the cDNA GFLN1 (Rosenthal and Gilly, 1993) were used. mRNA corresponding to this gene is expressed widely throughout the squid nervous system (Liu and Gilly, 1995).

Polyclonal antisera (produced in collaboration with Dr. S.R. Levinson, University of Colorado) were raised against a bacterial fusion protein that contained amino acids (aa) 483-576 of the predicted GFLN1 sequence. These residues compose the C-terminal half of the cytoplasmic linker between domains I and II. Construction of the fusion protein is described in detail elsewhere (Rosenthal, 1996). Polyclonal antisera ($Ab_{483\text{-}576}$) were affinity-purified using the soluble fraction of the fusion protein coupled to an affinity column (AminoLink, Pierce) according to manufacturer's protocol.

A monoclonal antibody ($mAb_{1305\text{-}21}$) was produced in collaboration with J. Burkhard and S. L. Feng, University of California, San Francisco. This antibody was directed against a synthetic peptide (synthesized by the Protein and Nucleic Acid Facility, Stanford University, Stanford, CA) corresponding to aa 1305-1321 of the GFLN1 sequence. These residues make up the part of the cytoplasmic linker between domains III and IV that is well conserved in most sodium channels (Gordon *et al.*, 1988).

Preparation of protein samples. Specificity of the antibodies was tested with tissue samples of cleaned giant axons and giant fiber lobes (GFL) taken from adult squid. Animals were rapidly decapitated before tissues were dissected in cold, Ca-free artificial seawater (480 m*M* NaCl, 10 m*M* $MgCl_2$, 5 m*M* EGTA, 10 m*M* HEPES, pH 7.4) for biochemical analysis. Segments of stellar nerves were ligated and cleaned by manually stripping off the small nerve fibers under microscopic observation until only the giant axon and its Schwann-cell sheath remained. Cleaned axons were cut at both ends and immediately placed in ice-cold lysis buffer containing proteinase inhibitors (Knudson *et al.*, 1989). Several axons were pooled, homogenized in the same buffer, and centrifuged at $1500 \times g$ for 10 min at 4°C. The supernatant was then used for protein-concentration analysis (bicinchoninic acid assay; Pierce, Rockford, IL) and for immunoblotting. Giant fiber lobe, brain, and cornea tissues were dissected and homogenized in the lysis buffer as described above. The resulting supernatant was centrifuged at $100{,}000 \times g$ for 30 min at 4°C to form a crude membrane pellet. This pellet was resuspended in lysis buffer for determination of protein concentration and for immunoblotting.

Muscle samples were obtained from animals anesthetized in 0.5% urethane in artificial seawater and dissected in cold, Ca-free artificial seawater. Thereafter, all muscle tissue was processed as described for giant fiber lobes (see above). To test for Na-channel protein within individual layers of circular mantle muscle, tissue samples from superficial and central layers were dissected and processed separately (outer and inner superficial layers were pooled). To test for the presence of Na-channel protein in the mantle muscle mass during post-hatching development, samples were taken from skinned mantles of hatchling and juvenile squid at four maturity stages (3 days, 2 weeks, 3 weeks, and 14 weeks) and from adults.

Immunoblotting. Protein samples (10 μg of total protein per lane) were separated by standard SDS-PAGE electrophoresis using 5% gels and transferred to nitrocel-

lulose. Nonspecific binding of the antibodies was minimized by pretreating the nitrocellulose with 10% nonfat dry milk in PBS (0.08 *M* Na_2HPO_4, 0.02 *M* NaH_2PO_4, 0.1 *M* NaCl) at pH 7.4. Affinity-purified antibodies were diluted as specified in the figure legends. Undiluted hybridoma supernatant was used as a source of monoclonal antibody. Goat anti-rabbit or goat anti-mouse secondary antibodies conjugated to horseradish peroxidase (Sigma) were used at 1:5000 dilution in conjunction with an enhanced chemiluminescence detection system (Renaissance, Du Pont NEN Research Products). For control experiments with blocked $Ab_{483-576}$, purified antiserum was incubated overnight at 4°C with the fusion protein antigen at a concentration of 0.1 mg/ml.

Results

Structural aspects of muscle fiber maturation

Squid hatchlings (1–2 days old) already possess the overall organization of radial and circular muscle fibers shown by adults (Bone *et al.*, 1995). Profiles of two distinct types of circular muscle fibers are visible in a longitudinal mantle section (Fig. 1A). Layers of superficial, large-diameter fibers on the outer and inner mantle surface enclose a central layer composed of fibers of smaller diameter. The superficial fibers and the central fibers differ in their mitochondrial content. In any given cross section, superficial mitochondria-rich (SMR) fibers often contain several large mitochondria, whereas central mitochondria-poor (CMP) fibers rarely display more than a single small one (Fig. 1). In both fiber types, the mitochondria are surrounded by loosely packed myofilaments (Fig. 1B, C). Myofilaments are rather poorly organized at this time, and sizable areas of cytoplasm without myofilaments are common. Similarly, the SR network is poorly developed and organized at this stage, with only a few SR tubules scattered among the myofilaments (Fig. 1B, C). Fibers of both types display very large nuclei (Fig. 1A).

By 8 weeks after hatching, several of the above characteristics show signs of substantial maturation. In addition to their difference in size and mitochondrial content (see also below), SMR and CMP fibers now clearly display differences in the organization of their myofilaments and SR (Fig. 2). The myofilament density increases considerably in both fiber types, but CMP fibers show a much thicker myofilament zone, both in absolute size and in relation to the mitochondrial core (Figs. 2B, 2C, and 3). Moreover, myofilaments in each fiber type are now organized in a characteristic manner. In cross sections of CMP fibers, myofilaments are divided by the SR and the Z-bodies into radially oriented, trapezoidal blocks (Fig. 2C). In the same sections, SMR fibers lack such divisions, and the myofilaments form a continuous ring around the central mitochondrial core (Fig. 2B). This difference between CMP and SMR fibers was found in cross sections examined at all maturity stages from week 1 on.

Longitudinal sections confirm the difference in width of the myofilament zone in relation to the mitochondrial core of the two circular fiber types (Fig. 3). These sections also reveal differences in myofilament staggering in the two fiber types. In CMP fibers, the myofilaments and Z-bodies form an oblique pattern across the fiber, which characterizes them as regular, obliquely striated muscles similar to those in other cephalopods (Gonzalez-Santander and Garcia-Blanco, 1972; Amsellem and Nicaise, 1980, Kier, 1985). In contrast, the myofilaments and Z-bodies of SMR fibers are lined up nearly in register across the fiber (Fig. 3). Although the appearance of the SMR fibers in cross section and longitudinal section is suggestive of cross striation rather than oblique striation, further morphological studies are necessary to clarify this point. The degree of myofilament staggering in a given section depends on the sectioning angle and on the degree of contraction of the muscle fiber (Rosenbluth, 1972; Kier 1985).

In all maturity stages, numerous profiles of neuronal processes containing round, clear vesicles were found (Fig. 4). These processes contact CMP and SMR muscle fibers at presumptive chemical synapses with clefts about 20 nm wide (Fig. 4C). A rich, ramifying network of these processes exists within the zone of CMP fibers, and individual processes appear to contact multiple fibers (Fig. 4A, B). Within the SMR fiber zone, nerve processes are less prominent and appear to run in grooves of the muscle fibers (Fig. 4D). The cross-sectional areas of synaptic vesicles were measured at a magnification of 240,000 on scanned micrographs, and vesicle diameters were calculated by assuming a spherical shape. Vesicles from processes associated with SMR fibers (mean diameter of 39 nm ± 0.7 SEM) are significantly smaller than those from processes associated with CMP fibers (mean diameter of 45.8 nm ± 0.6 SEM). These values are significantly different by Student's *t* test ($df = 225$, $P < 0.005$).

Quantitative aspects of muscle fiber maturation

In longitudinal sections, the circular mantle muscle mass is divided by bands of radial fibers into rectangular muscle segments (Figs. 1A and 2A). The dimensions of such a muscle segment, in a given section, can be described by (i) its thickness (*i.e.*, the distance between the outer and inner tunics) and (ii) its width (*i.e.*, the distance between two successive radial-fiber bands). Horizontal sections through the entire body of a juvenile showed that the thickness and the width of the muscle segments

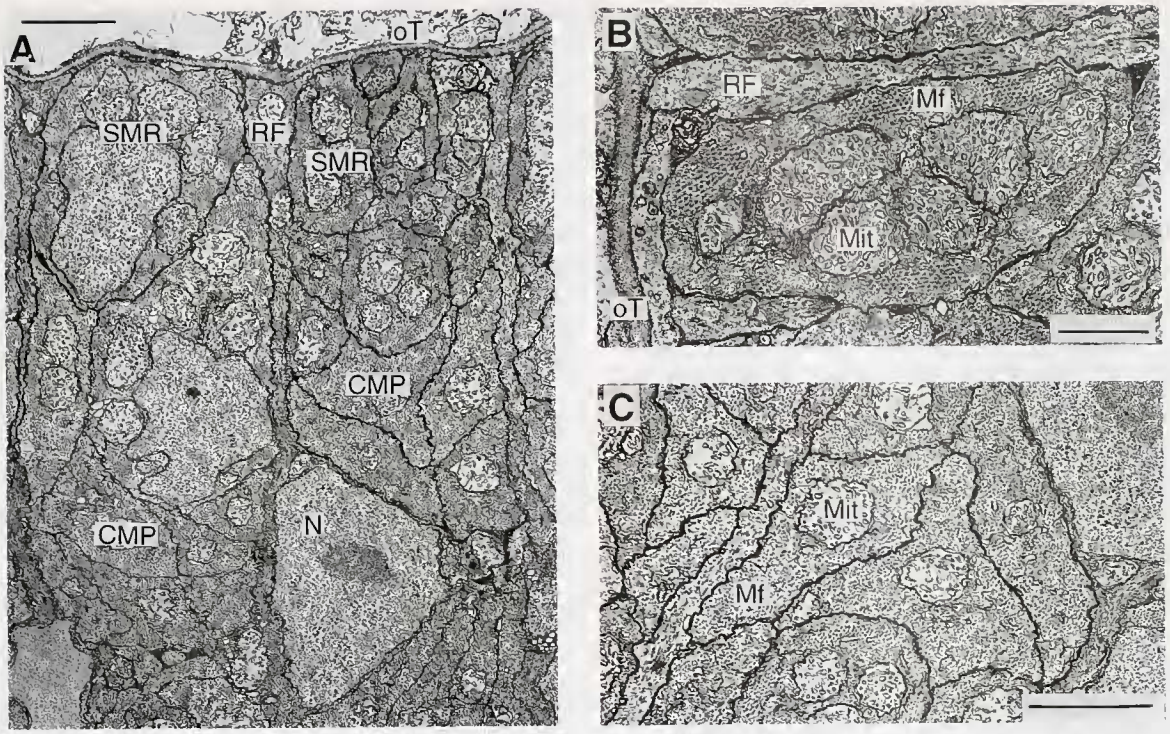

Figure 1. Transmission electron micrographs of superficial (outer) and central layers of mantle muscle from a squid hatchling (1–2 days old). (A) Cross section of circular muscle fibers showing the outer layer composed of 1–2 superficial mitochondria-rich fibers (SMR) and half of the central zone composed of mitochondria-poor fibers (CMP). Radial fibers (RF; cut longitudinally) divide mantle muscle into rectangular segments. N = nucleus; oT = outer tunics. Scale bar = 2 μm. (B) Cross section of a single SMR fiber. Many large mitochondria (Mit) are located in the central core. Mf = myofilaments. Scale bar = 1 μm. (C) Cross section of several CMP fibers. Usually one mitochondrion is located in the central core of an individual CMP fiber. Note the irregular shape of CMP fibers and the lack of any myofilament organization. Scale bar = 2 μm.

vary considerably along the mantle. The thickest and widest segments are found about one-third of the way from the anterior mantle end, whereas more anterior and posterior segments become progressively thinner and narrower. Transverse mantle sections, on the other hand, show almost no variation in the thickness of the muscle segments in a given section, although segments become very narrow dorsally at the location of the pen. In light of these results, the mantle region that contains the thickest muscle segments was chosen for analyzing the growth of the mantle muscle, and two animals of each age group with similar dorsal mantle length (DML) were studied.

In adults, muscle segments from this same area of the mantle were analyzed. Although adult animals were part of a spawning population, only very robust males that showed no sign of skin damage or senescence were studied. We therefore consider it unlikely that any selective "deconstruction" of the mantle muscle mass took place prior to fixation (Giese, 1969; O'Dor and Wells, 1978).

A muscle segment in a hatchling (2 mm DML) encloses the profiles of about 20–22 circular muscle fibers, of which 12–14 are CMP fibers (*i.e.*, $\approx$ 60%). During growth, the number of fibers enclosed in a single muscle segment increases considerably, but SMR and CMP fibers increase at different rates (Fig. 5). By 8 weeks (12 mm DML), the number of CMP fibers has increased about 10-fold, whereas the number of SMR fibers increases only 2.5-fold (Fig. 5A). Thus, the relative proportion of CMP fibers increases during growth (Fig. 5B), and by week 8, about 84% of the fibers in a muscle segment are CMP fibers. This proportion is comparable to that derived from analysis of a single muscle segment in a mature animal (110 mm DML; muscle segment 2.8 $\times$ 0.12 mm), which revealed a total of about 12,000 circular fibers, 86% of which were CMP fibers (Fig. 5A, B).

Morphometric measurements on the ultrastructural level for developing CMP fibers are summarized in Figure 6A. Mean cross-sectional area of CMP fibers doubles between 1 week and 8 weeks of age and increases by a

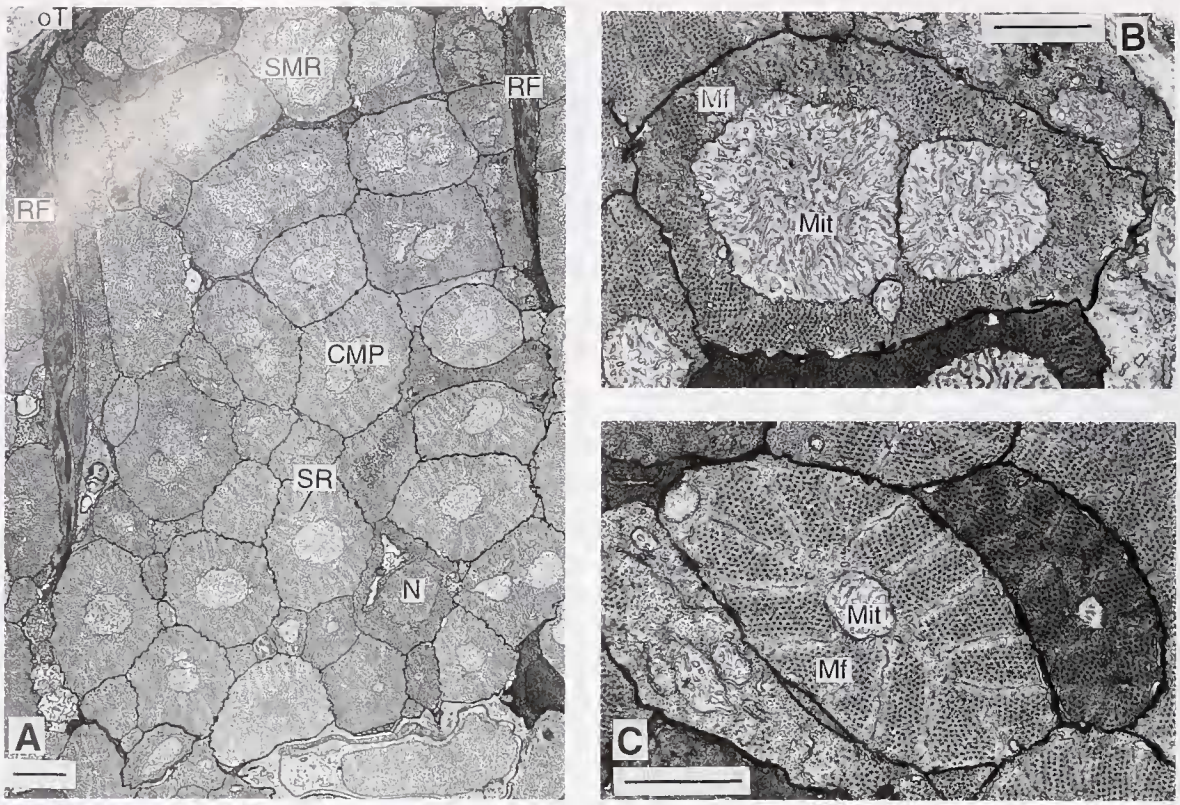

Figure 2. Transmission electron micrographs of superficial (outer) and central layers of mantle muscles from a juvenile squid (8 weeks old). (A) Cross section of circular muscle fibers showing the outer layer composed of several SMR fibers and part of the central zone composed of CMP fibers. Radial fibers (RF) are cut longitudinally. CMP fibers show a well-developed sarcoplasmic reticulum (SR). oT = outer tunics. Scale bar = 2 μm. (B) Cross section of a single SMR fiber. A continuous ring of myofilaments (Mf) surrounds a massive core of large mitochondria (Mit). Scale bar = 1 μm. (C) Cross section of a single CMP fiber. The myofilament area is divided into trapezoidal blocks by SR and Z-bodies. Only a small proportion of the fiber is occupied by mitochondria (Mit). Scale bar = 1 μm.

total of 3- to 4-fold in mature animals. This increase in fiber cross-sectional area is almost exclusively due to an increase in the filament and SR area. The mitochondrial core contributes relatively little to the absolute fiber size and, moreover, does not grow in proportion to the rest of the fiber. As a consequence, the relative area occupied by the mitochondrial core in CMP fibers decreases during growth from 16.3% ± 0.6% SEM in 1-week-old animals to 6% ± 0.3% SEM in adults.

In Figure 6B, results of the same ultrastructural analysis are presented for SMR fibers. The mean cross-sectional area of SMR fibers shows a pattern of increase similar to that described above for CMP fibers, although the absolute fiber area is much larger in SMR fibers (Fig. 6A, B left). Growth in SMR fibers, however, reflects a substantial increase in both the filament and SR area and the mitochondrial core. As a result, the proportional area occupied by the mitochondrial core in SMR fibers remains more-or-less constant at about 40%.

Functional maturation of circular muscle fibers in locomotion

The anatomical data described above indicate that the circular muscle of the mantle changes in composition during post-hatching maturation. At hatching, SMR and CMP fibers contribute almost equally to the circular mantle mass. Subsequent growth is mostly due to an increase in the contribution of CMP fibers, and the relative contribution of SMR fibers to the mantle mass in an adult is only about 14%. These structural changes suggest that the mantles of hatchlings and adults may have different contractile and endurance properties. For example, the endurance capabilities of SMR fibers should be manifested in respiration-related slow swimming (Bone *et al.*, 1995) or hovering (Zuev, 1966), and their relative contribution to jet-propelled locomotion should be most apparent at the earliest stages of maturation. To test this idea, we compared the kinematics of mantle

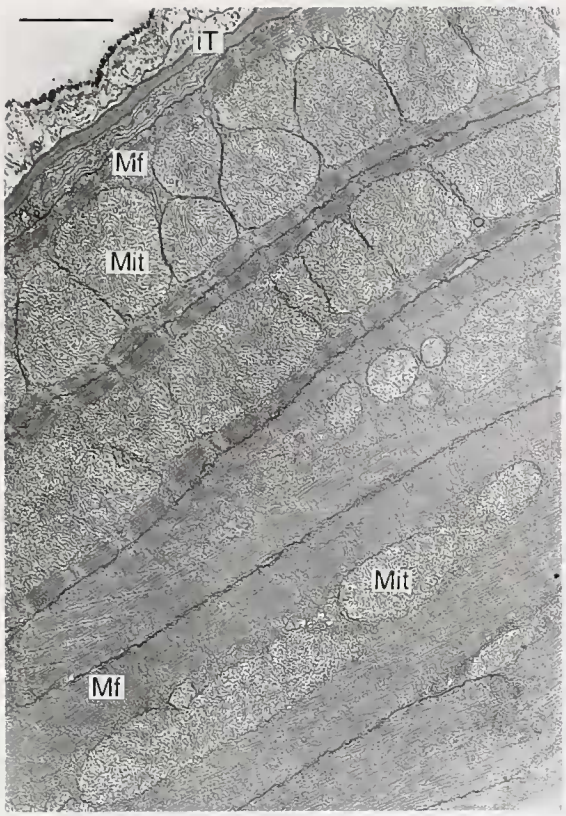

Figure 3. Transmission electron micrograph of mantle muscle fibers from a juvenile squid (8 weeks old). Longitudinal section of circular muscle fibers showing portions of two SMR fibers and three CMP fibers. Note the differences in mitochondrial content and in myofilament (MF) staggering angle between SMR and CMP fibers. Mit = mitochondria; iT = inner tunics. Scale bar = 2 μm.

contractions in freely swimming 1-week-old and adult squid during hovering behavior.

Adults and juveniles show quite different locomotor behavior during hovering. Adults move slowly back and forth, either in a slightly head-down or head-up position, due to gentle jets and undulatory fin movements. Juveniles, on the other hand, continuously bob up and down in a definite head-down position. Although juveniles beat their very small fins rapidly (up to 16 Hz), locomotion at this stage is apparently driven primarily by jetting. Comparison of the mantle kinematics in Figure 7 shows that hovering juveniles (2.5 mm DML) produce jets about twice as frequently (2.7 Hz) as do adults (1.3 Hz). In addition, the fractional change in mantle diameter in juveniles (≈32%) is about three times that in adults (≈12%; Fig. 7).

Identification of Na-channel protein in developing mantle muscle

Both Na-channel antibodies described in this study were produced against predicted sequence for the putative squid Na channel encoded by the cDNA GFLN1 (Rosenthal and Gilly, 1993). mRNA corresponding to GFLN1 is expressed throughout the squid nervous system, particularly in neurons, including those of the GFL, whose axons are large, long, or both (Liu and Gilly, 1995). These tissues were therefore used to test the specificity of the Na-channel antibodies.

Results of the monoclonal antibody $mAb_{1305\text{-}21}$ with GFL and cleaned axon samples are shown in Figure 8A. A prominent band with an apparent molecular weight of about 250 kD is present in both lanes. Control experiments with secondary antibody alone gave no signal (not illustrated). Similar results were obtained using the polyclonal antibody $Ab_{483\text{-}576}$ with GFL samples (Fig. 8B). In this case, a control experiment employing blocked-$Ab_{483\text{-}576}$ (see Methods) demonstrates specificity. The specificity of these antibodies for Na-channel protein is also supported by the fact that both antibodies give similar results, even though they are directed against two distinct portions of the protein encoded by GFLN1.

As detected by the polyclonal antibody, a specific (*i.e.*, blockable) Na-channel band centered around 210–220 kD is prominent in protein samples derived from mantle muscle (Fig. 8C). The monoclonal antibody also recognizes a comparable band in muscle tissue (not illustrated). Thus, it appears that Na-channel protein is relatively abundant in mantle muscle tissue.

Results obtained with a control tissue expected to show minimal Na-channel protein are also shown in Figure 8C. The cornea of the eye is a simple arrangement of a layer of epithelial cells supported by a transparent layer of muscle fibers (unpubl. obs.). Whole-cell patch clamp recordings made, using established methods (Gilly *et al.*, 1990, 1996), from enzymatically dissociated cells from both layers failed to reveal the presence of any voltage-gated Na currents (unpubl. results); the immunoblot results also fail to reveal a strong Na-channel band (Fig. 8C). The weak bands in the cornea lane may arise from axonal membrane, because the muscle fiber layer of the cornea presumably is innervated. These bands are blocked in the control experiment (Fig. 8C).

Electrophysiological recordings of Na currents in circular muscle fibers of squid mantle have been reported, and it was proposed that the muscle fibers with Na currents were small-diameter, CMP fibers (Gilly *et al.*, 1996). To test this idea, mantle tissue was dissected from an adult squid (see Methods) to provide samples of pure CMP circular fibers (plus radial fibers) and samples containing SMR fibers (plus contaminating CMP fibers as well as radial fibers). The results of an immunoblot with these samples are shown in Figure 9. The Na-channel band is most prominent in the central-zone sample,

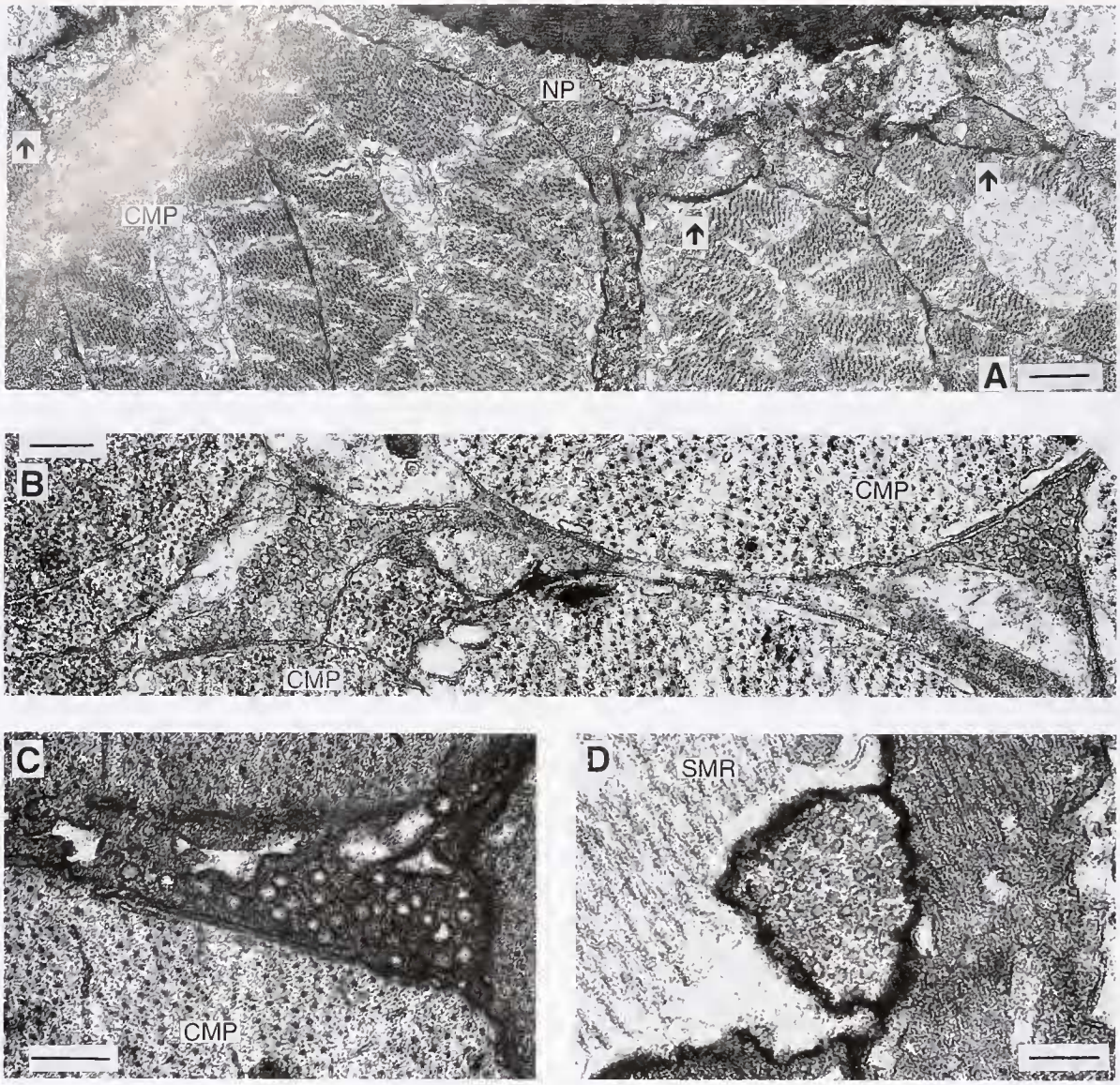

Figure 4. Transmission electron micrographs of synaptic profiles contacting circular mantle muscle fibers (juvenile; 8 weeks old). (A and B) Longitudinal mantle section (circular fibers in cross section). A nerve process (NP) runs within the central muscle layer and forms putative synaptic contacts (arrows) onto several CMP fibers. Note the relatively large dimensions of the synaptic profiles in relation to the size of the muscle fiber. (C) Neuromuscular junction onto a CMP fiber. The synaptic profile is filled with round, clear vesicles. (D) Synaptic profile running within a groove of an SMR fiber. Scale bars = 0.5 μm for A, and 0.2 μm for B–D.

much weaker in the superficial (inner/outer) sample, and quite strong in the whole-mantle sample.

If Na channels are preferentially expressed in CMP fibers, the relative abundance of Na-channel protein in whole-mantle samples should increase during the post-hatching period of maturation described in this study. Mantle samples were therefore collected from squid during this period and processed for immunoblotting. Results in Figure 10 confirm the predicted pattern. The muscle-type Na-channel band of low apparent molecular weight (relative to the neuronal form detected in brain; see also Fig. 8A) increases steadily in intensity between days 3 and 100 post-hatching. At this latter time, the band is comparable to that in the adult squid. Because each lane in Figure 10 was loaded with the same amount of protein, these results strongly suggest that the

relative abundance of Na-channel protein in mantle muscle is increasing during maturation.

Discussion

Comparison of the histology of the circular muscle of squid mantle during development from hatchling to adult reveals large changes in the size and number of the muscle fibers. Moreover, clear changes in the relative proportions of the different types of fiber are associated with maturation; these, in turn, affect mantle kinematics and jet-propelled locomotion.

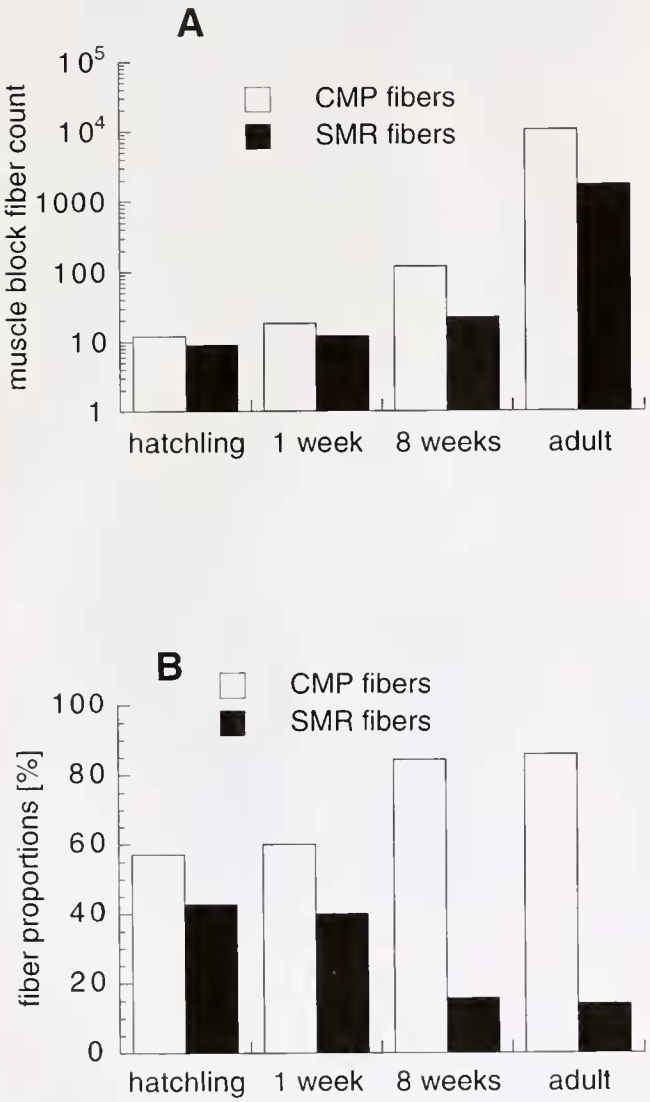

Figure 5. Recruitment of CMP and SMR fibers during mantle growth. (A) Absolute fiber counts are from individual muscle segments from hatchling, 1-week-old, 8-week-old, and adult squid. (B) Histogram of relative proportion of SMR and CMP fibers at different maturity stages.

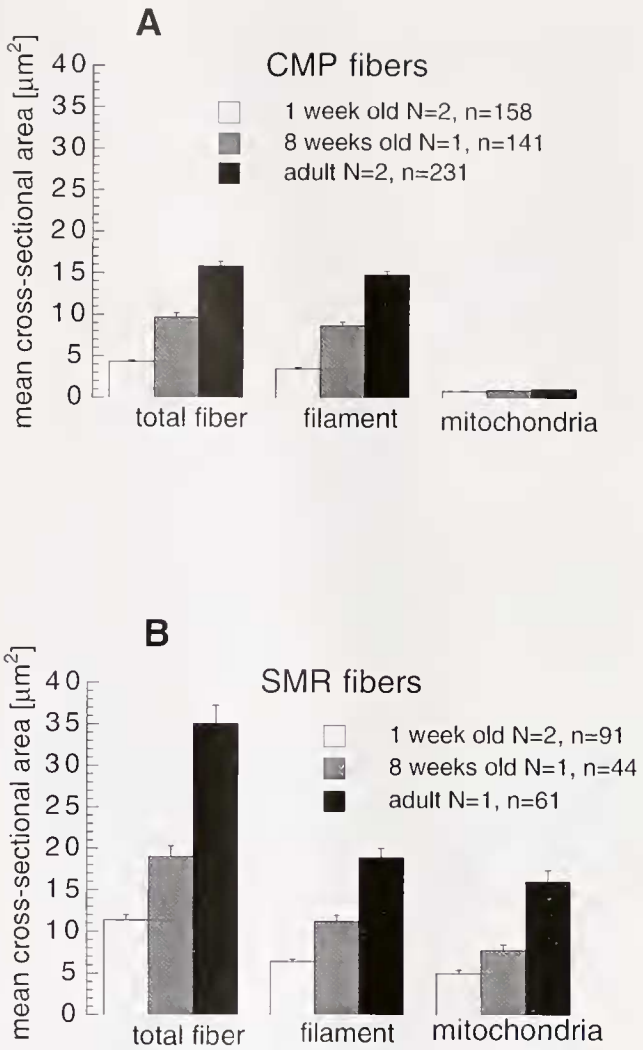

Figure 6. Characteristics of muscle fiber growth in CMP (A) and SMR (B) fibers. Individual histograms are given for the total cross-sectional fiber area, the filament and SR area, and the area occupied by the mitochondrial core for three maturity stages (means ± SEM; N = number of animals; n = number of measurements).

Mantle growth in squid is due to an increase in the size of existing muscle fibers (hypertrophy) and to recruitment of new fibers (hyperplasia). The extensive increase in fiber number in a single muscle segment, however, suggests that the latter mechanism is dominant in overall growth, and may also be responsible for the rapid somatic growth rates reported in squid (Forsythe and Van Heukelem, 1987). Similar growth mechanisms have been found in other squid (Moltschaniwskyj, 1994) and in teleost fish (Weatherley *et al.*, 1988).

On an ultrastructural level, hypertrophy in both SMR and CMP fibers is based on a steady increase in the number of myofilaments and, in the case of SMR fibers, the

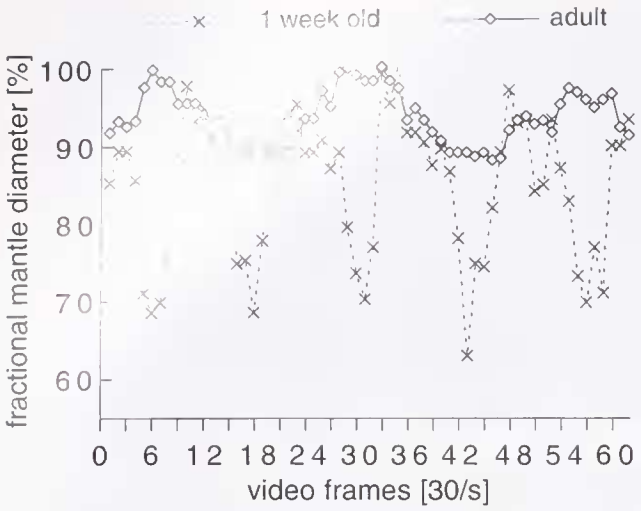

Figure 7. Mantle kinematics analyzed from video recordings of hovering or slow-swimming adult and juvenile squid. Mantle diameter was measured at the widest point (dorsal view), and the fractional mantle diameter was calculated by defining the largest diameter in a given measurement sequence as 100%. Time resolution is 30 frames/s.

size of the mitochondrial core. CMP fibers, however, show a selective hypertrophy of the myofilament and SR area and thus add a disproportional amount of force-generating capability at the individual fiber level. Nevertheless, hypertrophy of individual muscle fibers is limited by physiological constraints. For example, fibers requiring rapid excitation-contraction coupling in the absence of a transverse tubular system need to be small in diameter (Bone and Ryan, 1973; Bone *et al.*, 1995). This constraint would especially affect the presumptive fast-twitch CMP fibers with their high myofilament volume-to-surface ratio (Fig. 2). Such limitations on fiber diameter would indeed necessitate extensive recruitment of new CMP fibers (Fig. 5) to maintain rapid muscular responses as an animal grows throughout development.

Two biochemical results described in this paper support the idea that at least some CMP fibers display Na-channel-based excitability. Such excitability is consistent with the hypothesis that these are fast-twitch fibers responsible for all-or-none mantle contractions (Young, 1938; Gilly *et al.*, 1996). The first supporting evidence is that Na-channel protein is primarily expressed in the CMP fiber layer. Second, the increase of Na-channel protein seen in developing mantle is comparable to the selective hypertrophy and hyperplasia of CMP muscle fibers as shown by histology. The Na-channel band in muscle tissue is of lower apparent molecular weight than that detected in neuronal tissue (Figs. 8–10), and this suggests that a distinct Na-channel isoform exists in muscle. The exact relationship of this Na channel to the GFLN1-derived channels, which have a predicted core-polypeptide mass of 203 kD, is currently unknown.

Nerve terminals have been previously described in the mantle of other squid (Bone *et al.*, 1981, 1982, 1995) and

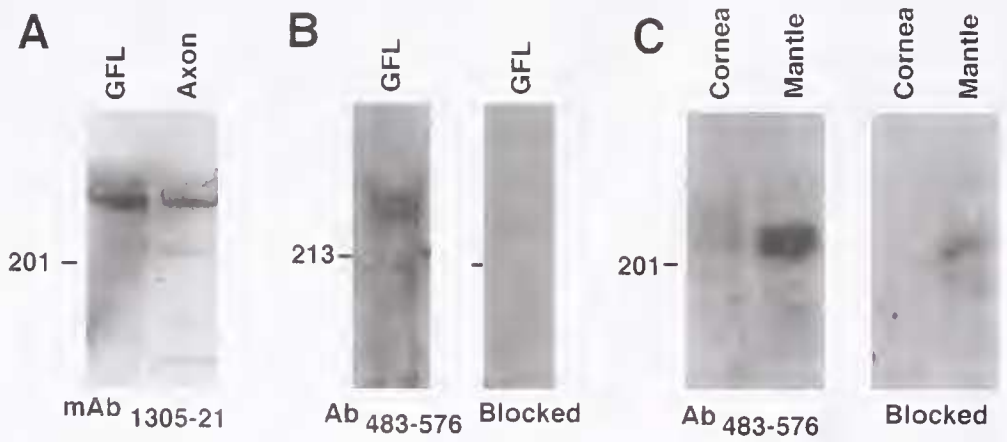

Figure 8. Specificity of Na-channel antibodies determined with immunoblots of samples of giant fiber lobe (GFL), cleaned giant axon, cornea, and mantle muscle. (A) $mAb_{1305\text{-}21}$ was used as undiluted hybridoma supernatant. Secondary goat anti-mouse antibody dilution was 1:5000. (B) $Ab_{483\text{-}576}$ was used at 1:1000 dilution, while dilution of secondary goat anti-rabbit antibody was 1:10,000. (C) $Ab_{483\text{-}576}$ used at 1:2000, dilution of secondary goat anti-rabbit antibody was 1:5000. Samples were prepared as described and separated on 5% SDS-PAGE gels. Each lane was loaded with 10 μg of total protein. Following transfer and antibody incubation, bands were detected by chemiluminescence reagent. A 260–280 kD band is detected in GFL and clean axon by monoclonal (A) and polyclonal (B) antibodies. A specific 210–220 kD band is present in mantle muscle, but not in cornea tissue (C). Blocking control was carried out as described in Methods.

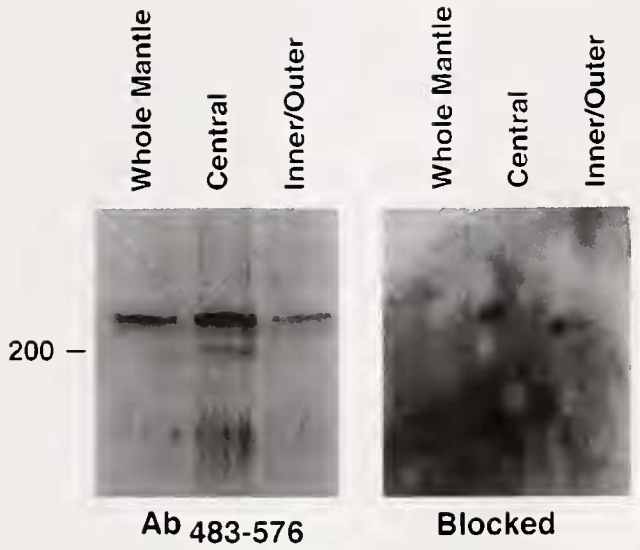

Figure 9. Identification of Na-channel protein in different layers of mantle muscle. Mantle muscle blocks were dissected to represent CMP fibers, SMR fibers, and whole mantle samples. $Ab_{483-576}$ was used at 1:1000 dilution; secondary goat anti-rabbit antibody dilution was 1:5000. Blocking control was prepared as described in Methods. Each lane was loaded with 10 μg of total protein. A 210–220 kD blockable band is detected in all samples. The band is most prominent in the CMP fiber sample, weaker in the SMR fiber sample, and strong in the whole-mantle sample. Although the CMP sample contains no SMR fibers, the SMR sample does contain some CMP fibers.

in other muscles of *Sepia* and *Octopus* (Graziadei, 1966). Although there is no direct evidence, the likely functional relationship between giant axons and CMP fibers (see above) and the large size of the neuronal processes contacting multiple CMP fibers (Fig. 4A, B) suggest that these processes may be the terminal branches of the giant axons. The origin of the terminal branches found within the SMR fibers remains unknown. Nevertheless, the detection of distinct size populations of vesicles in nerve profiles associated either with CMP or SMR fibers is consistent with the idea that different types of motor axons innervate the two fiber types (Bone *et al.*, 1981).

Muscle fiber recruitment takes place at different rates in CMP and SMR fibers during maturation; *i.e.*, the relative proportions of SMR to CMP fibers change progressively from 1:1 in hatchlings to 1:6 in adults. SMR fibers possess a high relative abundance of mitochondria (Figs 1–3) and a high content of oxidative enzymes (Mommsen *et al.*, 1981), which suggests that hatchlings and juveniles may have a higher demand for aerobic, fatigue-resistant muscles than do adults. This is consistent with our findings that the frequency and extent of mantle contractions during hovering (slow swimming) are substantially higher in juveniles than in adults (Fig. 7). These differences undoubtedly reflect the fact that juveniles are more negatively buoyant than adults (Zuev, 1966), and that, in contrast to adults, fin beating plays only a minor role during hovering (and for locomotion in general; v. Boletzky, 1982; Hoar *et al.*, 1994).

The disproportional increase of CMP fibers, on the other hand, suggests a higher demand for acceleration power in adults than in juveniles. It is clear that CMP fibers are necessary to produce the fast and powerful mantle contractions required for the high accelerations seen during escape- and attack-jets in all maturity stages (Gilly *et al.*, 1991). Indeed, Packard (1969) showed that acceleration power increases during development in *Loligo* (*i.e.*, an increase of power per unit weight of mantle muscle during escape-jets), which would be consistent with the disproportional increase of CMP fibers described in the present study.

The disproportional increase of CMP fibers may also reflect metabolic constraints due to the restricted capacity of hemocyanin to deliver oxygen (Wells, 1983; O'Dor *et al.*, 1990). This might effectively limit the proportion of aerobic SMR fibers in the mantle that can be supplied with oxygen (O'Dor, 1988), despite the heavy vascularization of this layer (Bone *et al.*, 1981). Even considering the fact that SMR fibers can be supplied with oxygen directly by diffusion through the skin (Wells and Wells, 1983; Pörtner, 1994), the size of the SMR fiber layer that

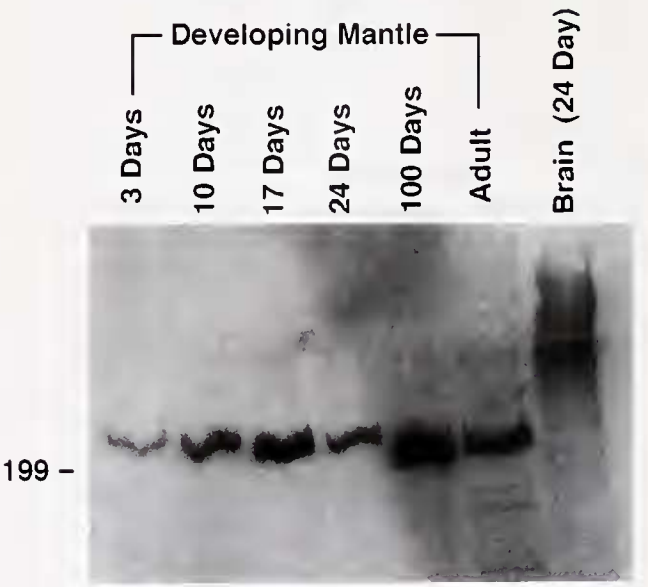

Figure 10. Apparent increase in abundance of Na-channel protein in developing mantle muscle. Mantle samples were collected from maturing squid and processed as described. In addition, a brain sample was included. $Ab_{483-576}$ was used in 1:1000 dilution, secondary antibody dilution was 1:5000. Each lane was loaded with 10 μg of total protein. The muscle samples show a 210–220 kD band of increasing intensity, whereas the brain sample shows a 260–280 kD band.

can thus be ventilated will be restricted. These constraints would again favor the recruitment of anaerobic CMP fibers during growth.

A final factor influencing the different ratios of SMR and CMP fibers found in hatchlings and adults pertains to growth-related changes in the forces acting on the body of a squid during jet-propelled swimming such as drag, thrust, and acceleration (Johnson *et al.*, 1972). Indeed, hatchlings and adults live at regimes of low and high Reynolds number respectively (Hoar *et al.*, 1994; Moltschaniwskyj, 1995); which, in turn, determines the relative importance of viscous and inertial effects on the hydrodynamic resistance to motion (Blake, 1983). For example, the movement of hatchlings ceases almost immediately when jet-propelled thrust stops, whereas adults coast over a considerable distance with a single jet (unpubl. data). These observations are consistent with the idea that viscous forces dominate over inertial forces in hatchlings and vice versa in adults. Thus, to cover any distance efficiently, hatchlings have to jet continuously because they cannot coast and therefore have a higher demand for aerobic, fatigue-resistant muscles than do adults.

Increasing size, on the other hand, places an additional constraint on the developing mantle muscle if rapid acceleration is to be maintained during growth. Inertial resistance is proportional to body mass, which increases as the third power of DML. Driving muscle force, on the other hand, is proportional to myofilament cross-sectional area, which increases with the square of DML (Daniel and Webb, 1987). Consequently, a disproportionate increase in fast-twitch CMP fibers would lead to a greater driving force for a given body size and, by tending to compensate for the increased inertial resistance as an animal grows, would help to maintain proper accelerations during escape- and attack-jets.

Acknowledgments

This material is based upon work supported by the National Institutes of Health under Grant No. NS-17510-14 and by the National Science Foundation under Grant No IBN-9631511. We are also grateful to Gilbert Van Dykhuizen and Reginald C. Gary (Monterey Bay Aquarium, California) for providing juvenile squid and to Dr. M. W. Denny for helpful comments on the manuscript.

Literature Cited

Amsellem, J., and G. Nicaise. 1980. Ultrastructural study of muscle cells and their connections in the digestive tract of *Sepia officinalis*. *J. Ultrastruct. Cytol.* **12(2):** 219–231.

Blake, R. W. 1983. *Fish Locomotion.* Cambridge University Press, Cambridge.

Boletzky, S. v. 1982. Developmental aspects of the mantle complex in coleoid cephalopods. *Malacologia* **23(1):** 165–175.

Boletzky, S. v. 1987. Juvenile behaviour. Pp. 45–60 in *Cephalopod Life Cycles—Volume II—Comparative Reviews*, P. R. Boyle, ed. Academic Press, London.

Bone, Q., and K. P. Ryan. 1973. The structure and innervation of locomotor muscles of salps (Tunicata: Thalicea). *J. Mar. Biol. Assoc. U. K.* **53:** 873–883.

Bone, Q., A. Pulsford, and A. D. Chubb. 1981. Squid mantle muscle. *J. Mar. Biol. Assoc. U. K.* **61:** 327–342.

Bone, Q., A. Packard, and A. L. Pulsford. 1982. Cholinergic innervation of muscle fibres in squid. *J. Mar. Biol. Assoc. U. K.* **62:** 193–199.

Bone, Q., E. R. Brown, and M. Usher. 1995. The structure and physiology of cephalopod muscle fibers. Pp. 301–329 in *Cephalopod Neurobiology*, N. J. Abbott, R. Williamson, and L. Maddock, eds. Oxford University Press, New York.

Chen, D. S., G. Van Dykhuizen, J. Hodge, and W. F. Gilly. 1996. Ontogeny of copepod predation in juvenile squid *(Loligo opalescens)*. *Biol. Bull.* **190:** 69–81.

Daniel, T. L., and P. W. Webb. 1987. Physical determinants of locomotion. Pp. 343–369 in *Comparative Physiology: Life in Water and On Land*, P. Dejours, L. Bolis, C. R. Taylor, and E. R. Weibel, eds. IX-Liviana Press, Padova.

Forsythe, J. W., and W. F. Van Heukelem. 1987. Growth. Pp. 135–156 in *Cephalopod Life Cycles—Volume II—Comparative Reviews*, P. R. Boyle, ed. Academic Press, London.

Giese, A. C. 1969. A new approach to the biochemical composition of the mollusc body. *Oceanogr. Mar. Biol. Annu. Rev.* **7:** 175–229.

Gilly, W. F., M. T. Lucero, and F. T. Horrigan. 1990. Control of the spatial distribution of sodium channels in giant fiber lobe neurons of the squid. *Neuron* **5:** 663–674.

Gilly, W. F., B. Hopkins, and G. O. Mackie. 1991. Development of giant motor axons and neural control of escape responses in squid embryos and hatchlings. *Biol. Bull.* **180:** 209–220.

Gilly, W. F., T. Preuss, and M. B. McFarlane. 1996. All-or-none contraction and sodium channels in a subset of circular muscle fibers of squid mantle. *Biol. Bull.* **191:** 337–340.

Gonzalez-Santander, R., and E. S. Garcia-Blanco. 1972. Ultrastructure of the obliquely striated or pseudostriated muscle fibers of the cephalopods: *Sepia, Octopus* and *Eledone*. *J. Submicrosc. Cytol.* **4:** 233–245.

Gordon, D., D. Merrick, D. A. Wollner, and W. A. Catterall. 1988. Biochemical properties of sodium channels in a wide range of excitable tissues studied with site-directed antibodies. *Biochemistry* **27:** 7032–7038.

Gosline, J. M., J. D. Steeves, A. D. Harman, and M. E. DeMont. 1983. Patterns of circular and radial muscle activity in respiration and jetting of the squid *Loligo opalescens*. *J. Exp. Biol.* **104:** 97–109.

Graziadei, P. 1966. The ultrastructure of the motor nerve endings in the muscles of cephalopods. *J. Ultrastruct. Res.* **15:** 1–13.

Hoar, J. A., E. Sim, D. M. Webber, and R. K. O'Dor. 1994. The role of fins in the competition between squid and fish. Pp. 27–43 in *Mechanics and Physiology of Animal Swimming*, L. Maddock, Q. Bone, and J. M. V. Rayner, eds. Cambridge University Press, New York.

Johnson, W., P. D. Soden, and E. R. Trueman. 1972. A study in jet propulsion: an analysis of the motion of squid, *Loligo vulgaris*. *J. Exp. Biol.* **56:** 155–165.

Kier, W. M. 1985. The musculature of squid arms and tentacles: ultrastructural evidence for functional differences. *J. Morphol.* **185:** 223–239.

Kier, W. M. 1988. The arrangement and function of molluscan mus-

cle. Pp. 211–252 in *The Mollusca, Vol. II Form and Function*, E. R. Trueman and M. R. Clarke, eds. Academic Press, San Diego.

Knudson, C. M., N. Chandhari, A. H. Sharp, J. A. Powell, K. G. Beam, and K. P. Campbell. 1989. Specific absence of the α subunit of the dihydropyridine receptor in mice with muscular dysgenesis. *J. Biol. Chem.* **264:** 1345–1348.

Lin, T. I., and W. F. Gilly. 1995. Tissue distribution and subcellular localization of Na^+ channel mRNA in the nervous system of the squid *Loligo opalescens*. *Recept. Channels* **3:** 243–254.

Matsuno, A. 1987. Ultrastructural studies on developing oblique-striated muscle cells in the cuttlefish, *Sepiella japonica* Sasaki. *Zool. Sci* **4:** 53–59.

Moltschaniwskyj, N. A. 1994. Muscle tissue growth and muscle fibre dynamics in the tropical loliginid squid *Photololigo sp.* (Cephalopoda: Loliginidae). *Can. J. Fish. Aquat. Sci.* **51:** 830–835.

Moltschaniwskyj, N. A. 1995. Changes in shape associated with growth in the loliginid squid *Photololigo sp.* morphometric approach. *Can. J. Zool.* **73:** 1335–1343.

Mommsen, T. P., J. Ballantyne, D. MacDonald, J. Gosline, and P. W. Hochachka. 1981. Analogues of red and white muscle in squid mantle. *Proc. Natl. Acad. Sci. USA* **78:** 3274–3278.

O'Dor, R. K. 1988. Limitations on locomotor performance in squid. *J. Appl. Physiol.* **64(1):** 128–134.

O'Dor, R. K., and M. J. Wells. 1978. Reproduction versus somatic growth: hormonal control in *Octopus vulgaris*. *J. Exp. Biol.* **77:** 15–31.

O'Dor, R. K., E. A. Foy, P. L. Helm, and N. Balch. 1986. The locomotion and energetics of hatchling squid, *Illex illecebrosus*. *Amer. Malacol. Bull.* **4(1):** 55–60.

O'Dor, R. K., H. O. Pörtner, and R. E. Shadwick. 1990. Squid as elite athletes: locomotory, respiratory, and circulatory integration. Pp. 481–503 in *Squid As Experimental Animals*, D. L. Gilbert, W. J. Adelman, and J. M. Arnold, eds. Plenum Press, New York.

Packard, A. 1969. Jet propulsion and the giant fibre response of *Loligo*. *Nature* **221:** 875–877.

Pörtner, H. O. 1994. Coordination of metabolism, acid-base regulation and hemocyanin function in cephalopods. *Mar. Fresh. Behav. Physiol.* **25:** 131–148.

Rosenbluth, J. 1972. Obliquely striated muscle. Pp. 389–419 in *The Structure and Function of Muscle—Vol. 1*, G. H. Bourne, ed. Academic Press, New York.

Rosenthal, J. J. C. 1996. Molecular identification of the ion channels underlying the action potential in the squid giant axon. Ph. D. Thesis, Department of Biological Sciences, Stanford University.

Rosenthal, J. J. C., and W. F. Gilly. 1993. Amino acid sequence of a putative sodium channel expressed in the giant axon of the squid *Loligo opalescens*. *Proc. Natl. Acad. Sci. USA* **90:** 10026–10030.

Ward, D. V., and S. A. Wainwright. 1972. Locomotory aspects of squid mantle structure. *J. Zool. (Lond.)* **167:** 437–449.

Weatherley, A. H., H. S. Gill, and A. F. Lobo. 1988. Recruitment and maximal diameter of axial muscle fibers in teleosts and their relationship to somatic growth and ultimate size. *J. Fish Biol.* **33:** 851–859.

Wells, M. J. 1983. Circulation in cephalopods. Pp. 239–290 in *The Mollusca, Vol 5*, K. M. Wilbur, ed. Academic Press, London.

Wells, M. J. 1988. Mantle muscle and mantle cavity in cephalopods. Pp. 287–300 in *The Mollusca—Form and Function*, E. R. Trueman and M. R. Clarke, eds. Academic Press, San Diego.

Wells, M. J., and J. Wells. 1983. The circulatory response to acute hypoxia in *Octopus*. *J. Exp. Biol.* **104:** 59–71.

Young, J. Z. 1938. The functioning of the squid giant nerve fibres of the squid. *J. Exp. Biol.* **15:** 170–185.

Zuev, G. V. 1966. Characteristic features of the structure of cephalopod molluscs associated with controlled movements. *Fisheries Research Board of Canada Translation Series No. 1011 1968.*